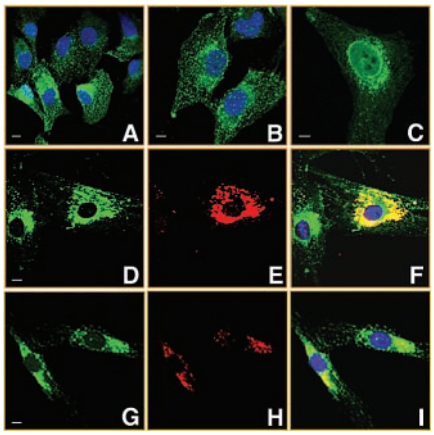

Fig. 3. Colocalization of optineurin with the Golgi apparatus. Immunocytochemistry assay and intracellular expression of optineurin in different human cell lines: (**A** to **C**) transformed cell lines and (**D** to **I**) primary dermal fibroblast cells. (A) HTM, (B) NPCE, and (C) HeLa. (D to F) Normal dermal fibroblast specific staining for (D) Golgi apparatus, (E) endogenous optineurin, and (F) superimposition of the two (yellow staining). (G to I) Dermal fibroblast of a glaucoma patient with an E50K mutation stained for (G) Golgi apparatus, (H) endogenous protein, and (I) superimposition of the two. Scale bars, 5 μm.

scription–polymerase chain reaction showed further expression in human trabecular meshwork (HTM), nonpigmented ciliary epithelium (NPCE), retina, brain, adrenal cortex, liver, fetus, lymphocyte, and fibroblast. Northern blotting revealed a major 2.0-kb transcript in HTM and NPCE and a minor 3.6-kb message that was three to four times less abundant (Fig. 2A).

Two different 18–amino acid peptides from the NH_2- and COOH-termini of optineurin were used to immunize chickens and to obtain antibodies to optineurin (*18*). The selected peptides are 100% conserved within human, mouse, and macaque. One of these antibodies cross reacted (*18*) with an ~66-kD protein in whole-cell extracts from a variety of cell lines (Fig. 2B). We also detected optineurin expression in aqueous humor samples of human, macaque, bovine, pig, goat, sheep, cat, and rabbit, suggesting that it is a secreted protein.

We next investigated the intracellular localization of optineurin by immunocytochemistry (*18*) using both primary and transformed cell lines. Endogenous optineurin showed granular staining that was associated with vesicular structures near the nucleus (Fig. 3, A to C, E, and H). The staining colocalized (Fig. 3, F and I) with a marker specific for the Golgi apparatus (Fig. 3, D and G). In a dermal fibroblast culture from a patient with an E50K mutation, optineurin was present at much lower levels than in a similar culture from a normal subject.

Optineurin has no significant homology to any protein, but it is known to interact with adenovirus E3-14.7K (*12*), Huntingtin (*15*), transcription factor IIIA (*16*), RAB8 (*17*), and two unknown kinases (*14*). Optineurin's ability to block the protective effect of E3-14.7K on tumor necrosis factor–α (TNF-α)–mediated cell killing suggests that this protein may be a component of the TNF-α signaling pathway that can shift the equilibrium toward induction of apoptosis (*12*). TNF-α can markedly increase the severity of damage in optic nerve heads of both POAG and LTG subjects (*20*, *21*). We speculate that wild-type optineurin, operating through the TNF-α pathway, plays a neuroprotective role in the eye and optic nerve, but when defective, it produces visual loss and optic neuropathy as typically seen in normal and high-pressure glaucoma.

Identification of *OPTN* as an adult-onset glaucoma gene provides an opportunity to study the biochemical pathways that may be involved in the pathogenesis of this group of optic neuropathies. In addition, because *OPTN* mutations are a contributing factor in patients with NPG, the gene may be a useful tool for presymptomatic screening of the general population.

References and Notes

1. H. A. Quigley, *Br. J. Ophthalmol.* **80**, 389 (1996).
2. H. A. Quigley, S. Vitale, *Invest. Ophthalmol. Vis. Sci.* **38**, 83 (1997).
3. J. M. Tielsch *et al.*, *JAMA* **266**, 369 (1991).
4. R. A. Hitchings, *Br. J. Ophthalmol.* **76**, 494 (1992).
5. C. Grosskreutz, P. A. Netland, *Int. Ophthalmol. Clin.* **34**, 173 (1994).
6. E. B. Werner, in *The Glaucomas*, R. Ritch, M. B. Shields, T. Krupin, Eds. (Mosby, St. Louis, MO, 1996), vol. 2, chap. 36.
7. R. A. Hitchings, S. A. Anderton, *Br. J. Ophthalmol.* **67**, 818 (1983).
8. M. Sarfarazi, *Hum. Mol. Genet.* **6**, 1667 (1997).
9. I. Stoilov, A. N. Akarsu, M. Sarfarazi, *Hum. Mol. Genet.* **6**, 641 (1997).
10. I. Stoilov *et al.*, *Am. J. Hum. Genet.* **62**, 573 (1998).
11. E. M. Stone *et al.*, *Science* **275**, 668 (1997).
12. Y. Li, J. Kang, M. S. Horwitz, *Mol. Cell. Biol.* **18**, 1601 (1998).
13. M. Sarfarazi *et al.*, *Am. J. Hum. Genet.* **62**, 641 (1998).
14. K. Schwamborn, R. Weil, G. Courtois, S. T. Whiteside, A. Israel, *J. Biol. Chem.* **275**, 22780 (2000).
15. P. W. Faber *et al.*, *Hum. Mol. Genet.* **7**, 1463 (1998).
16. R. J. Moreland *et al.*, *Nucleic Acids Res.* **28**, 1986 (2000).
17. K. Hattula, J. Peranen, *Curr. Biol.* **10**, 1603 (2000).
18. Supplementary Web material is available on *Science* Online at www.sciencemag.org/cgi/content/full/295/5557/1077/DC1.
19. T. Rezaie, M. Sarfarazi, unpublished data.
20. L. Yuan, A. H. Neufeld, *Glia* **32**, 42 (2000).
21. G. Tezel, M. B. Wax, *J. Neurosci.* **20**, 8693 (2000).
22. J. T. den Dunnen, S. E. Antonarakis, *Hum. Genet.* **109**, 121 (2001).
23. We thank P. Kaufman, J. Seeman, J. Suchecki, and T. Digiulio for aqueous humors and eye specimens and P. Reynolds for clinical evaluation and interpretation of patients' notes. M.S. is supported by grants from the National Eye Institute (EY-09947), the International Glaucoma Association (IGA-G249), and the University of Connecticut General Clinical Research Center (M01-RR-06192). A.C. is supported by Bluff Field Charitable Trust U.K., the International Glaucoma Association, and St. George's Hospital Medical School and National Health Service Trust. G.B. is supported by the Royal National Institute for the Blind.

5 October 2001; accepted 28 December 2001

Methyltransferase Recruitment and DNA Hypermethylation of Target Promoters by an Oncogenic Transcription Factor

Luciano Di Croce,[1]* Veronica A. Raker,[1] Massimo Corsaro,[1] Francesco Fazi,[2] Mirco Fanelli,[1,5] Mario Faretta,[1] Francois Fuks,[4] Francesco Lo Coco,[3] Tony Kouzarides,[4] Clara Nervi,[2] Saverio Minucci,[1] Pier Giuseppe Pelicci[1,6]*

DNA methylation of tumor suppressor genes is a frequent mechanism of transcriptional silencing in cancer. The molecular mechanisms underlying the specificity of methylation are unknown. We report here that the leukemia-promoting PML-RAR fusion protein induces gene hypermethylation and silencing by recruiting DNA methyltransferases to target promoters and that hypermethylation contributes to its leukemogenic potential. Retinoic acid treatment induces promoter demethylation, gene reexpression, and reversion of the transformed phenotype. These results establish a mechanistic link between genetic and epigenetic changes during transformation and suggest that hypermethylation contributes to the early steps of carcinogenesis.

Cancer cells present global hypomethylation of the genome and hypermethylation of islands of CpG dinucleotide clusters within specific DNA regions (*1*–*3*). Although overexpression of DNA methyltransferases (Dnmt's) has been proposed as a mechanism for aberrant genome methylation, it does not explain the specific regional hypermethyl-

ation in cancer cells. PML-RAR is an oncogenic transcription factor found in acute promyelocytic leukemias (APLs) (*4*–*6*). Using PML-RAR as a paradigm for an oncoprotein, we examined whether PML-RAR is responsible for CpG methylation of its target genes and whether aberrant methylation is relevant for its biological activity.

PML-RAR functions as a transcriptional regulator of retinoic acid (RA) target genes (*7*–*9*). Among its putative targets, we focused on the RA receptor RARβ2, because it contains a CpG island and is considered to be a putative tumor suppressor (*10*).

Chromatin immunoprecipitation (ChIP) analysis of PR9 (U937 hemopoietic precursors carrying the PML-RAR cDNA under a zinc-inducible promoter) and control (MT) cells (*11*) revealed that PML-RAR is bound to the endogenous RARβ2 promoter in vivo, irrespective of the presence of RA, its natural ligand (Fig. 1A). Transient transfection of PML-RAR and an RARβ2 promoter–luciferase reporter gene (RARβ-Luc) (*12*) revealed a dose-dependent repressive effect of the fusion protein on RARβ2 transcription (Fig. 1B). Although RARβ2 was expressed in untreated PR9 cells and normal hematopoietic precursors ($CD34^+$) (Fig. 1D), it was not expressed in zinc-treated PR9 cells (as early as 8 hours after induction of PML-RAR expression) (Fig. 1C), in blasts from four APL patients, or in the APL-derived NB4 cell line (Fig. 1D). These findings indicate that PML-RAR binds to the RARβ2 promoter and induces its transcriptional silencing.

To investigate RARβ2 methylation in PML-RAR–expressing cells, we analyzed a CpG-rich region that comprises the RARβ2 promoter and the 5′ portion of the exon 1 by bisulfite sequencing, using eight randomly selected alleles from each APL sample type. In untreated PR9 cells, the frequency of 5-methylcytosine residues was approximately 9% (Fig. 1E, 0 hours). Expression of PML-RAR induced further methylation of this region, which was evident as early as 4 to 8 hours (18 to 22%), and peaked at 48 hours (50%), after induction. Promoters that contain a CpG island but no RAR elements (RAREs) (such as that of p66shc) (*13*) were not modified by PML-RAR expression (*14*). Comparable high frequencies of 5-methylcytosine residues were found in NB4 cells and in three APL samples (Fig. 1E) (*15*). Methylation-specific polymerase chain reaction (PCR) (*16*) revealed methylation of the 5′ portion of the RARβ2 exon 1 in seven out of nine APL samples, but not in $CD34^+$ cells (*15*). The minimum region of methylation found in all APL samples lies within the RARβ2 exon 1, at one nucleosome distance from the RARβ2 RARE and the TATA box (Fig. 1E). Its methylation correlates with RARβ2 silencing in breast cancers (*17*).

We next investigated whether PML-RAR–induced methylation of RARβ2 is responsible for its transcriptional silencing. In vitro methylation of the cloned RARβ2 promoter, by either the Sss I or the Hpa II methylase, reduced its basal activity by about 85% (Fig. 1B) (*14*). Only a single CpG–Hpa II methylation site is present within the iden-

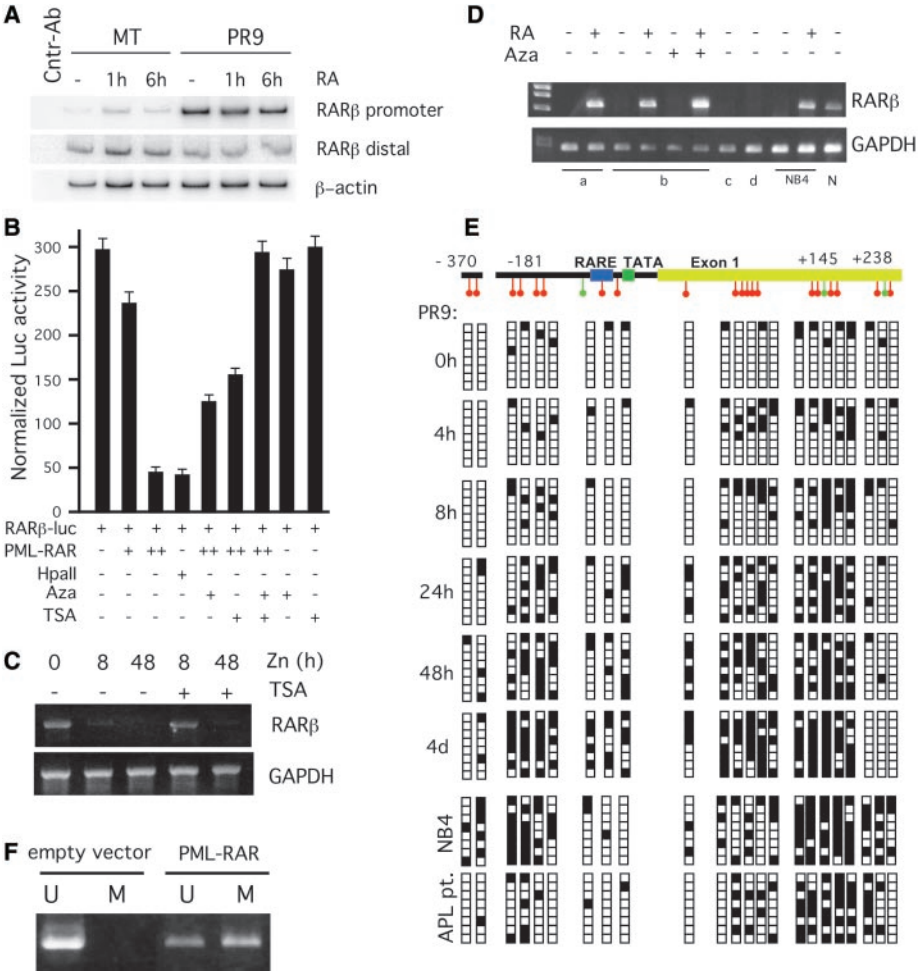

Fig. 1. PML-RAR causes RARβ2 promoter hypermethylation and silencing. (**A**) PML-RAR binds to the RARβ2 promoter. PR9 and control MT cells (which carry an empty inducible vector) were exposed to $ZnSO_4$ (Zn) (*11*) and RA. ChIP analysis was performed with antibodies to PML (PGM3) or an unrelated (Cntr-Ab) antibody (*28*). RARβ2 promoter and distal sequences were amplified by polymerase chain reaction (PCR) under linear conditions. (**B**) Human embryonic kidney 293T cells were transiently transfected with RARβ-luc and PML-RAR 24 hours before luciferase activity measurement. TSA (100 nM) and 5-Aza-dC (1 μM) were added, as indicated. The RARβ2 promoter was methylated in vitro with Hpa II before addition, as indicated. (**C**) PML-RAR represses RARβ2 expression. Total RNA was extracted from PR9 cells either untreated or treated with Zn for 8 or 48 hours, and analyzed by reverse transcription (RT)–PCR. (**D**) RARβ2 is silenced in APL blasts. Blasts from four APL patients (a through d) or NB4 cells were treated with RA or 5-Aza-dC, as indicated, and analyzed by RT-PCR. N, $CD34^+$ cells. (**E**) Methylation status of the RARβ2 promoter. Genomic DNA from PR9, an APL patient, or NB4 cells were subjected to sodium bisulphite modification, and the RARβ2 promoter was amplified as described (*17*). To avoid differential amplification of methylated versus unmethylated CpGs, primers did not contain CpG dimers. Circles, CpG dinucleotides; green circles, Hpa II methylation sites; black and white squares, methylated and unmethylated CpGs, respectively. (**F**) Methylation-specific PCR of ectopically expressed RARβ2 promoter. 293T cells were cotransfected with RARβ-luc and PML-RAR or an empty vector. Recovered plasmids were subjected to sodium bisulphite treatment and amplified with primers specific for methylated (M) (RARb5′, 5-gtcgagaacgcgagcgattc-3; and LUC3′; 5-acgaataaaataacgccga-3) or unmethylated (U) (RARb5′, 5-gatgttgagattgtgagtgattt-3; and LUC3′; 5-acaaataaaataacaccaa-3) DNA.

[1]Department of Experimental Oncology, European Institute of Oncology, Milan, Italy. [2]Department of Histology and Medical Embryology, [3]Department of Cellular Biotechnology and Hematology, University of Rome, "La Sapienza," Rome, Italy. [4]Wellcome/CRC Institute and Department of Pathology, Cambridge University, Cambridge, UK. [5]Department of Morphological Science, University of Camerino, Italy. [6]Italian Foundation for Cancer Research (FIRC) Institute for Molecular Oncology, Milan, Italy.

*To whom correspondence should be addressed. E-mail: ldicroce@lar.ieo.it (L.D.C.); pgpelicci@ieo.it (P.G.P.)

tified common region of methylation (Fig. 1E). PML-RAR–induced methylation of the cotransfected RARβ2 promoter (Fig. 1F) and treatment with the methylation inhibitor 5-Aza-dC significantly reduced RARβ2-luc repression by transfected PML-RAR (Fig. 1B). Thus, DNA methylation contributes to the repressive effect of PML-RAR on RARβ2 transcription.

We investigated whether PML-RAR associates with specific DNA methyltransferases, such as Dnmt1 or Dnmt3a (*18*, *19*). Co-immunoprecipitation experiments revealed a physical association between PML-RAR and endogenous Dnmt1 or Dnmt3a in both PR9 and NB4 cells (Fig. 2, A and B). ChIP analysis of overexpressed proteins revealed that Dnmt1 and Dnmt3a were specifically enriched at the RARβ2 promoter in the presence of PML-RAR (Fig. 2, C and D), demonstrating that PML-RAR and Dnmt's form stable complexes on the RARβ2 promoter.

PML-RAR expression disrupts the integrity of the PML nuclear bodies (NBs) and delocalizes several NB proteins to hundreds of punctated structures, so-called microspeckles (Fig. 2E). In the absence of PML-RAR, both Dnmt1 and Dnmt3a are nuclear diffuse, whereas in cells expressing PML-RAR, Dnmt1 and Dnmt3a were delocalized to the PML-RAR microspeckles (Fig. 2E) (*15*). Thus, PML-RAR expression alters the nuclear compartmentalization of Dnmt's and recruits them to the newly formed PML-RAR microspeckles.

We mapped the Dnmt3a binding sites within PML-RAR. Overexpressed Dnmt3a formed a stable complex with PML (Fig. 2F) but not with RAR (*14*) or RAR-RXR (Fig. 2G). Because the PML moiety leads to oligomerization, we tested a chimeric protein containing RAR and the p53-tetramerization domain (p53-RAR) (*20*) for interactions with Dnmt's. Dnmt3a interacted with p53-RAR (Fig. 2G),

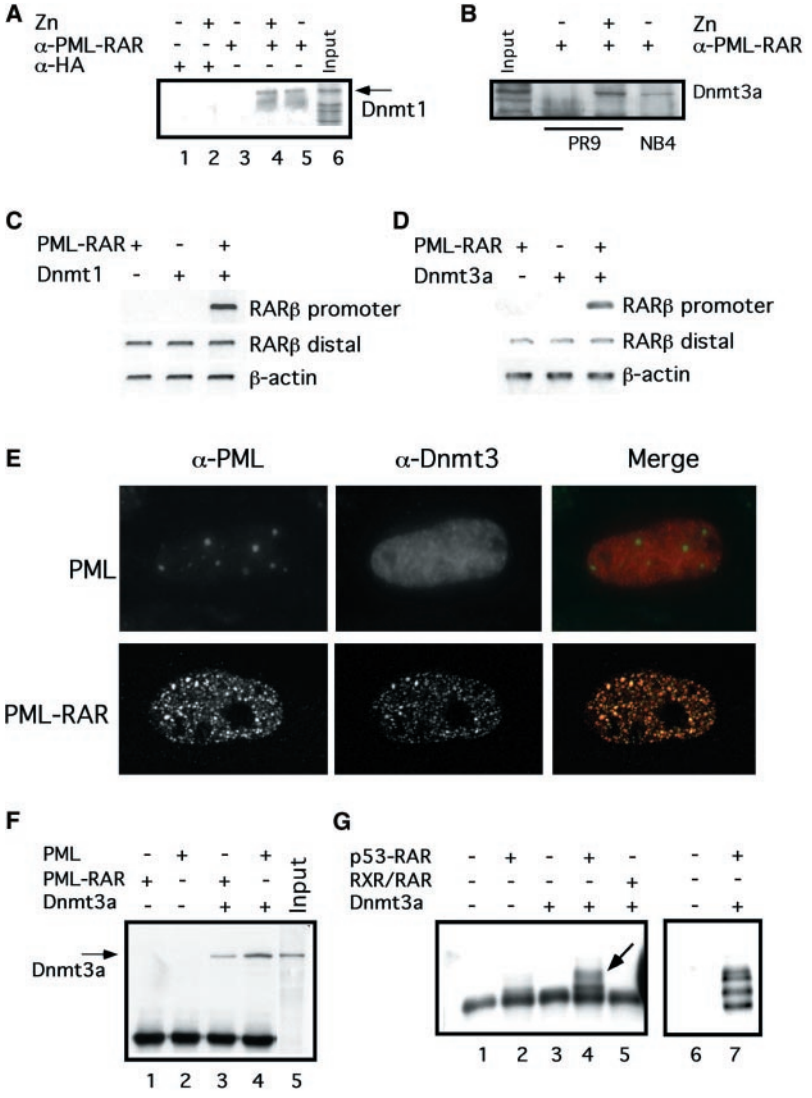

Fig. 2. Dnmt's interact with PML-RAR. (**A** and **B**) NB4 [(A), lanes 1 and 5; (B), as indicated] and PR9 [(A), lanes 2 through 4 and lane 6; (B), as indicated] cells were treated, or not, with Zn and were cross-linked with 0.5 mM 3,3′-dithiobisproprionamidate-2-HCl. Nuclear extracts (*28*) were immunoprecipitated with the PGM3 or control antibody to hemagglutinin (HA) and probed with the antibody to Dnmt1 (A) or the antibody to Dnmt3a (B). (**C** and **D**) PML-RAR recruits Dnmt's to the RARβ2 promoter. PML-RAR and/or myc-Dnmt1 (C) or myc-Dnmt3a (D) were transiently transfected into 293T cells. ChIP was performed as described in Fig. 1A, using a monoclonal antibody to Myc. (**E**) Immunofluorescent localization of PML, PML-RAR, and myc-Dnmt3a in human HEL 299 cells. Representative confocal laser scanning microscopy images are shown (*29*). Merges highlight areas of co-localization (yellow). (**F** and **G**) 293T cells were transiently transfected as indicated. Dnmt3a was myc-tagged. Cell lysates (*27*) were precipitated with PGM3 (F), antibody to Myc [(G), left panel] or antibody to RAR [(G), right panel]. Western blots were probed with an antibody to Myc (F) or to RAR (G). The arrow indicates co-precipitated p53-RAR (G).

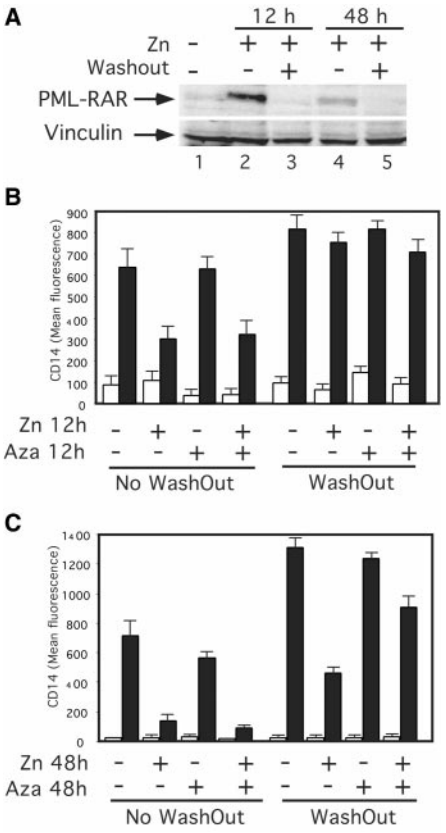

Fig. 3. Epigenetic role of PML-RAR in differentiation. (**A**) PR9 cells were untreated (lane 1) or treated with Zn for 12 hours (lanes 2 and 3) or 48 hours (lanes 4 and 5). Zn was washed out in lanes 3 and 5. Western blots of cell lysates were analyzed with the PGM3 antibody. (**B** and **C**) PR9 cells were untreated or treated with Zn, 5-Aza-dC, or a combination of these for 12 hours (B) or 48 hours (C). Zn was washed out from half the cells (washout), and cells were allowed to recover for 24 hours. VD (250 ng/ml) and transforming growth factor–β (1 ng/ml) were then added for 36 hours (black bars). Cell differentiation was monitored by flow cytometry of the differentiation antigen CD14, as previously described (*4*). Error bars represent the SD from the mean of triplicate experiments.

suggesting that RAR, in the context of the PML-RAR multimeric complex, contributes to the formation of PML-RAR/Dnmt complexes. PML-RAR, therefore, establishes multiple interactions with Dnmt's, through both its PML and RAR moieties.

We next asked whether the epigenetic modifications mediated by PML-RAR contribute to its biological activities. PML-RAR exerts opposing effects on differentiation: inhibitory, in the absence of RA; and stimulatory, in the presence of pharmacological doses of RA. Mechanistically, recruitment of the histone deacetylase (HDAC) complex by PML-RAR is critical for its ability to repress transcription and block differentiation (*5*). Accordingly, RA treatment leads to dissociation of the PML-RAR/HDAC complex, conversion of PML-RAR into a transcriptional activator, and differentiation of APL blasts (*5*, *6*). Zinc treatment of PR9 cells for 12 or 48 hours blocked Vitamin D3–induced differentiation (Fig. 3B). Removal of zinc from the culture medium (washout) led to the rapid disappearance of PML-RAR expression (within 24 hours) (Fig. 3A). The PML-RAR–induced differentiation block could be reverted by zinc washout after a 12-hour, but not 48-hour, exposure to PML-RAR (Fig. 3C). Differentiation block induced by transient (48 hours) exposure to PML-RAR was prevented by 5-Aza-dC (Fig. 3C). Thus, transient PML-RAR expression suffices to induce epigenetic changes that render cells permanently refractory to differentiation. However, 5-Aza-dC treatment was unable to prevent the PML-RAR–induced differentiation block when PML-RAR was continuously expressed (no washout) (Fig. 3C). This suggests that PML-RAR represses transcription and blocks differentiation through two independent and temporally distinct mechanisms: (i) recruitment of HDAC (via the RAR moiety) (*5*, *6*), and (ii) recruitment of Dnmt's (through the PML moiety) and subsequent promoter methylation. This dual behavior is consistent with our observations that: (i) PML-RAR–induced repression of RARβ2 transcription was only partially released by either 5-Aza-dC or the HDAC inhibitor trichostatin A (TSA) but was completely released by simultaneous treatment (Fig. 1B); (ii) RARβ2 was silenced as early as 8 hours after PML-RAR expression, despite incomplete promoter methylation (Fig. 1, C and E); and (iii) RARβ2 transcription was restored by TSA treatment at early (8 hours), but not late (48 hours), time points (Fig. 1C). Similarly, in APL samples, RARβ2 transcription was not induced by TSA alone but was induced by the combination of TSA, 5-Aza-dC, and RA (*15*). A synergistic effect of TSA and 5-Aza-dC in restoring gene expression has been observed for other cancers (*21*).

We investigated whether the RARβ2 promoter is demethylated during RA-induced differentiation of APLs. In NB4 cells, treatment with RA and 5-Aza-dC decreased the frequency of 5-methylcytosine residues by approximately 50% when given individually and by 75% when given simultaneously (Fig. 4A). Similar results were observed with blasts from three APL patients or with zinc-induced PR9 cells (*14*, *15*). RA treatment led to an accumulation of RARβ2 mRNA in both APL blasts and NB4 cells (Fig. 1D). Co-treatment with RA and 5-Aza-dC led to a further increase in the RARβ2 mRNA level, whereas 5-Aza-dC alone had no effect (Figs. 1D and 4B). These findings establish a tight correlation among RARβ2 demethylation and reexpression and induction of differentiation (Fig. 4C).

Our results suggest a scenario in which oncogenic transcription factors aberrantly recruit Dnmt's to target promoters. Newly methylated CpGs then become docking sites for methyl-binding proteins, which in turn interact with both HDAC complexes and Dnmt's (*22*, *23*). The assembled complexes could be further stabilized by interactions between Dnmt's and HDAC1 (*24*, *25*). If the initial recruitment step is not prevented, it may eventually lead to spreading of hypermethylation to the neighboring regions, locking these into a stably silenced chromatin state.

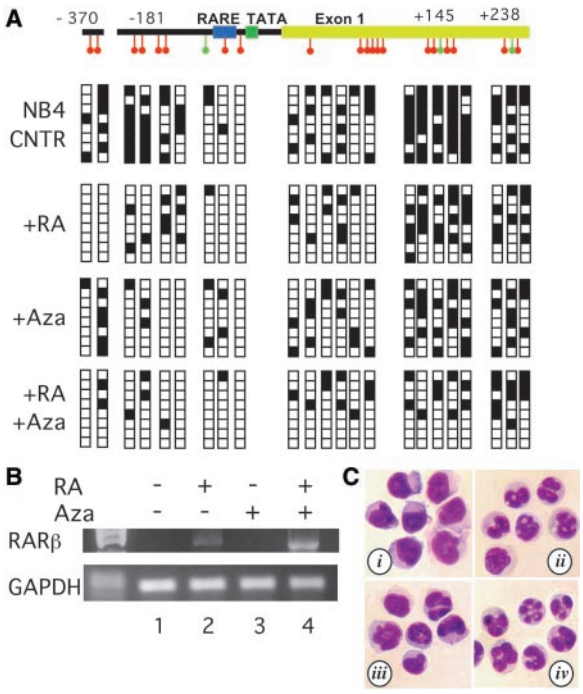

Fig. 4. Methylation status of the RARβ2 promoter in NB4 cells. (**A**) Bisulphite genomic sequencing was performed as in Fig. 1E. RA or 5-Aza-dC was added for 48 hours. (**B**) NB4 cells were untreated or treated for 48 hours with RA or 5-Aza-dC, as indicated. RT-PCR of RARβ2 expression was performed as described in Fig. 1C. GAPDH, glyceraldehyde phosphate dehydrogenase. (**C**) Wright-Giemsa staining of blasts isolated from a newly diagnosed APL patient either untreated (i) or treated for 48 hours with RA (ii) or 5-Aza-dC (iii) or a combination of these (iv).

References and Notes

1. A. P. Bird, A. P. Wolffe, *Cell* **99**, 451 (1999).
2. P. A. Jones, P. W. Laird, *Nature Genet.* **21**, 163 (1999).
3. S. B. Baylin, J. G. Herman, *Trends Genet.* **16**, 168 (2000).
4. F. Grignani *et al.*, *Cell* **74**, 423 (1993).
5. F. Grignani *et al.*, *Nature* **391**, 815 (1998).
6. R. J. Lin *et al.*, *Nature* **391**, 811 (1998).
7. T. Casini, P. G. Pelicci, *Oncogene* **18**, 3235 (1999).
8. L. Benedetti *et al.*, *Blood* **87**, 1939 (1996).
9. M. Ruthardt *et al.*, *Mol. Cell. Biol.* **17**, 4859 (1997).
10. R. L. Momparler, V. Bovenzi, *J. Cell. Physiol.* **183**, 145 (2000).
11. F. Grignani *et al.*, *EMBO J.* **15**, 4949 (1996).
12. H. de The, M. M. Vivanco-Ruiz, P. Tiollais, H. Stunnenberg, A. Dejean, *Nature* **343**, 177 (1990).
13. P. G. Pelicci, unpublished data.
14. L. Di Croce *et al.*, data not shown.
15. Supplementary Web material is available on *Science* Online at www.sciencemag.org/cgi/content/full/295/5557/1079/DC1.
16. J. G. Herman, J. R. Graff, S. Myohanen, B. D. Nelkin, S. B. Baylin, *Proc. Natl. Acad. Sci. U.S.A.* **93**, 9821 (1996).
17. M. Widschwendter *et al.*, *J. Natl. Cancer Inst.* **92**, 826 (2000).
18. T. Bestor, A. Laudano, R. Mattaliano, V. Ingram, *J. Mol. Biol.* **203**, 971 (1988).
19. M. Okano, S. Xie, E. Li, *Nature Genet.* **19**, 219 (1998).
20. S. Minucci *et al.*, *Mol. Cell* **5**, 811 (2000).
21. E. E. Cameron, K. E. Bachman, S. Myohanen, J. G. Herman, S. B. Baylin, *Nature Genet.* **21**, 103 (1999).
22. P. S. Knoepfler, R. N. Eisenman, *Cell* **99**, 447 (1999).
23. L. Di Croce, unpublished data.
24. F. Fuks, W. A. Burgers, A. Brehm, L. Hughes-Davies, T. Kouzarides, *Nature Genet.* **24**, 88 (2000).
25. K. D. Robertson *et al.*, *Nature Genet.* **25**, 338 (2000).
26. V. Orlando, H. Strutt, R. Paro, *Methods* **11**, 205 (1997).
27. M. Alcalay *et al.*, *Mol. Cell. Biol.* **18**, 1084 (1998).
28. MT and PR9 cells were labeled with (5′-^{3}H)-thymidine for 24 hours, treated with 100 μM $ZnSO_4$ for 16 hours, treated with 1 μM RA for 1 or 6 hours, and then cross-linked (*26*). Cross-linked DNA was immunoprecipitated and recovered (*27*) and used to amplify a 346–base pair RARβ2 promoter region (from –203 to +143) containing the RARE.
29. Confocal microscopy was performed with a BIORAD MRC1024ES kripton-argon laser scanning confocal microscope, attached to an inverted Olympus microscope IX70.

30. We thank M. Beato for helpful discussions, the FIRC Institute of Molecular Oncology sequencing facility, Roche-Italia for the vitamin D_3 supply, and A. Bird and E. Li for antibodies and plasmids. L.D.C. was supported by a FIRC–European Oncology Foundation fellowship and a J. Carreras Foundation–European Hematology Association fellowship, and V.A.R. was supported by a European Union (EU) Marie Curie Fellowship. This work was supported by EU (BMH4-CT98-3745), FIRC, and Italian Association for grants.

7 August 2001; accepted 2 January 2002